Bioresource Technology Reports 24 (2023) 101682

Contents lists available at ScienceDirect

Bioresource Technology Reports

journal homepage: www.sciencedirect.com/journal/bioresource-technology-reports

Outdoor pilot-scale cultivation and techno economic assessment of a novel omega-3 eicosapentaenoic acid over-producing *Nannochloropsis oculata* strain

Wan Aizuddin Wan Razali [a], Jagroop Pandhal [b,*]

[a] Faculty of Fisheries & Food Science, Universiti Malaysia Terengganu, 21030 Kuala Nerus, Terengganu, Malaysia
[b] Department of Chemical and Biological Engineering, University of Sheffield, Sheffield, United Kingdom

ARTICLE INFO

Keywords:
Microalgae
Biochemical analysis
High-value bioactive compounds
Omega-3 eicosapentaenoic acid (EPA)
Mutant strain

ABSTRACT

Nannochloropsis oculata is a microalga that produces a significant amount of eicosapentaenoic acid (EPA). Cultivating strains in photobioreactors commercially can be challenging. We cultivated a mutant *N. oculata* strain, capable of accumulating >40 % EPA more than the wild-type strain at laboratory scale, in an outdoor 300 L pilot-scale photobioreactor, in the U.K. The mutant *N. oculata* recorded the highest amount of EPA quantity at 129.87 mg/g dry cell weight (DCW) compared to the wild-type strain, which accumulated 75.43 mg/g DCW. A techno-economic assessment (TEA) evaluated the feasibility of the study. Using specific combined cultivation scenarios, the process resulted in a positive net present value (NPV) and return on investment (ROI) at £52,156,484.46 and 607.22 % after 10 years, respectively. The TEA of the improved EPA quantity by M1 *N. oculata* showed the high processing cost could be overcome by high yields and an optimised operational strategy.

1. Introduction

Microalgae represent an emerging sustainable source of bioactive products for the health market, including carotenoids, vitamins, and omega-3 (Kumar et al., 2022). The demand for nutraceutical products and super-functional foods is growing as people become more health-conscious (Ghosh et al., 2022; Paterson et al., 2023). Omega-3 eicosapentaenoic acid (EPA) is a notable component of microalgae that reduces the risk of chronic diseases such as cancer, heart disease, and arthritis, while also enhancing muscle metabolic flexibility and strength (Gammone et al., 2019). *N. oculata*, a unicellular oleaginous microalga, is one such species that has a relatively high EPA content (Sousa et al., 2022). Although low-cost fish and krill oils are presently the primary sources of omega-3 (Cecchin et al., 2022), the growing demand for fish and fish oil will require a more sustainable source, with microalgae the primary replacement candidates. However, the cost of the overall process needs to be reduced (Barros de Medeiros et al., 2022).

Currently, there is a focus on increasing the EPA content in specific microalgal strains. This is because the price range of microalgae oil falls between 80 and 160 USD per kg, and this variation is due to the quantity of omega-3 incorporated accumulated within the total oil, i.e. the price of microalgae oil correlates directly with the quantity of EPA (Schade and Meier, 2021). However, one of the primary challenges associated with producing EPA from microalgae is the significant expense incurred in cultivation and downstream processing. One solution is the biorefinery concept, and co-producing high-value-added products, such as protein, astaxanthin, and exopolysaccharides (Rafa et al., 2021).

Several studies have reported on the cultivation of different strains of wild-type *Nannochloropsis* at pilot scale, using natural source of light and heat to reduce cultivation costs. For instance, one study found that a strain of *N. oceanica* grown in a 6000 L outdoor pilot-scale raceway pond in Portugal produced an average of 26–29.5 % EPA of total fatty acids (TFA), which is comparable to other species of *Nannochloropsis* (Cunha et al., 2020). Another study, also in Portugal, reported that *N. gaditana*, cultured in a semi-continuous mode in a 100 L outdoor tubular photobioreactor, had an EPA content that reached 41.56 % of TFA (Nogueira et al., 2020). Moreover, the cultivation of *N. oceanica* in an outdoor (simulated) 5 L plastic-bag type photobioreactor resulted in an EPA quantity of 41.2 mg/g dry cell weight (DCW) (Chen et al., 2018). Additionally, *N. oculata* and *N. salina* have shown consistent growth productivity levels in outdoor photobioreactor systems, suggesting that these microalgae species are stable and resistant to environmental

* Corresponding author.
E-mail address: j.pandhal@sheffield.ac.uk (J. Pandhal).

https://doi.org/10.1016/j.biteb.2023.101682
Received 17 May 2023; Received in revised form 24 October 2023; Accepted 26 October 2023
Available online 29 October 2023

stresses (Quinn et al., 2012). Consequently, *Nannochloropsis* species are expected to thrive in outdoor photobioreactor systems and achieve optimal growth.

In this study, the performance of a high EPA-producing *N. oculata* mutant strain was assessed in a 300 L outdoor photobioreactor. This was undertaken to assess growth and productivity of the novel strain compared to the wild-type, using environmental light and temperature conditions. Generally, wild-type microalgae strains do not reach economic parity with fish oils in terms of EPA and DHA productivity (Chauton et al., 2015). The novel mutant strain (M1) was generated and characterised in a previous study using a chemical mutagenesis and novel selection methodology based on enzymatic inhibitors (Wan Razali et al., 2022). It was shown to accumulate 37.5 % EPA per TFA with a high productivity of 68.5 mg/g DCW.

The production of EPA was evaluated for its economic viability through a TEA analysis, incorporating the experimental findings of replicate outdoor cultivation experiments into a model previously developed by Schade and Meier (2021). Until recently, there have been limited published results on assessing the economic feasibility of the main industrial *Nannochloropsis* species. Furthermore, all studies have used predictive models to evaluate the technical and economic performance of *Nannochloropsis* species (Kang et al., 2019; Schade and Meier, 2021; Vázquez-Romero et al., 2022). However, a pilot-scale photobioreactor experiment provides a more accurate means of predicting the actual EPA content and improving the accuracy of developed TEA models. High-precision data is necessary to bridge the gap between the models' findings and the setup of future microalgae biorefinery plants. To determine the sustainability of the developed strain in the outdoor setup, economic measures such as net present value (NPV) and return on investment (ROI) were used.

2. Materials and methods

2.1. Materials and Methods

Wild-type strain *N. oculata* (849/1) from Culture Collection of Algae and Protozoa (CCAP) Scotland and EPA-overproducing M1 strain (Wan Razali et al., 2022), were cultured in an f/2 medium (Stein, 1979) with 33.5 g/L salinity of synthetic seawater (Instant Ocean® Sea Salt, United Kingdom). In brief, M1 *N. oculata* strain was developed by using ethyl methane sulfonate and screened using fatty acid synthase inhibitor, cerulenin and MGDG synthase inhibitor, galvestine-1 (Wan Razali et al., 2022). All the chemicals used in this study were purchased from Sigma-Aldrich, United Kingdom, unless otherwise specified.

A volume of 800 mL inoculum was started in 6 replicates of 1 L flasks photobioreactor, exposed to 150–200 μmol m^{-2} s^{-1} fluorescence light (Lumilux cool white fluorescent bulbs, Osram, United Kingdom) and the light intensity was measured using an LI-250A light sensor (LI-COR Bioscience, New England, USA). The microalga was cultured with 12 h light/dark cycles, 20 °C and standard aeration at 2 L/min. Once the optical density (OD) (λ = 595 nm) reached approximately 0.7 absorbance, 400 mL volume was transferred to two units of 20 L carboys that were exposed to the same growth conditions. 1 mL sample in triplicates were taken for each harvested stock batch microalga culture and observed using a microscope (BX51, Olympus, Japan) and ensure the microalgae cells were in the exponential growth phase (having the size around 3 μm) and dominating the culture over bacteria. The inoculum in the 1 L flasks was refreshed by adding f/2 sterile medium. The process was repeated until a 40 L microalga inoculum was obtained.

2.2. Description of pilot-scale photobioreactor

An outdoor 300 L pilot-scale PhycoFlow® photobioreactor was installed at Arthur Willis Environmental Centre (53.3832000157627° North, −1.4995194567741421° West), Department of Animal and Plant Sciences, University of Sheffield. The PhycoFlow® was encased in a Sunlite multiwall polycarbonate unit with 83 % light transmission (Leflay et al., 2020). The photobioreactor consisted of two stages, the photo stage and the dark stage. The photo stage comprises transparent glass tubes (length: 2.5 m; outer diameter: 54 mm; wall thickness: 1.8 mm) and u-bend glass tubes (width: 234 mm; outer diameter: 54 mm; wall thickness: 2.5 mm; height: 200 mm) connected by using compression twist couplers in a serpentine arrangement. The serpentine arrangement helps in reducing the pumping requirements and prevents biofilm build-up and contamination (Acién et al., 2017). The dark stage consisted of a 300 L holding tank, where the nutrient dosing line, PT 100 thermocouple, and negative temperature coefficient (NTC) probe for temperature measurement and pH probe were located. The photobioreactor has a heating and cooling system and uses an electric heater (Marko Electrical, United Kingdom) and a tap water sprayer (Varicon Aqua, United Kingdom) to maintain the temperature within the range of 10 to 30 °C. The CO_2 was supplied at the bottom of the holding tank and the initial point of the light stage. The photobioreactor is controlled by a system located next to the holding tank which includes a timer controller for aeration, solenoid operation for nutrient dosing, a water-powered injector system for cooling, a temperature and pH meter controller, a heating control circuit, a variable drive pump motor controller, a low-level protection circuit for the pump, heating, and cooling circuits, and buttons for starting and stopping the photobioreactor. A control system is housed in a waterproof, IP66-rated GRP enclosure.

The process of starting up the photobioreactor involved chemical sterilisation of the system by adding 3 L of 2 % sodium hypochlorite (Alfa Aesar, United Kingdom) to approximately 297 L of tap water. This created an available chlorine concentration of 200 mg/L, which was then circulated throughout the photobioreactor for a period of 24 h. After this time, 3.42 L of 5 % sodium thiosulphate (Thermo Fisher Scientific, United Kingdom) was used to neutralise the chlorine. The solution was then circulated for an additional 24 h before being drained to remove any remaining particles from the photobioreactor.

Before beginning the cultivation process, the holding tank was supplied with 270 L of tap water. Then, 10 kg of artificial seawater (Instant ocean, United Kingdom) was added to create an artificial seawater solution with salinity levels of 33.5 g/L. Next, 750 mL of 2 % sodium hypochlorite was added to create an available chlorine concentration of 50 mg/L, and the solution was circulated for 24 h. After that, 855 mL of 5 % sodium thiosulphate was added, and the solution was circulated for another 24 h. Finally, sterile nutrients were added to prepare f/2 medium (CCAP, Scotland) in the photobioreactor.

To begin the experiment, approximately 40 L of *N. oculata* in exponential phase with an OD of approximately 1.125 absorbance (λ = 595 nm) were added to the prepared f/2 medium in a 300 L photobioreactor to achieve an initial culture concentration of around 0.15 measured at 595 nm. The culture was circulated for 24 h at a flow velocity of approximately 0.42 m/s using a CO4–350/02 K 3-phase SS pump (ITT Lowara, United Kingdom). Pure CO_2 was supplied daily to maintain a pH range of 7–8.5. Wild-type and M1 strains *N. oculata* were supplied with 4.5 % and 4 % CO_2 (v/v), respectively, throughout 15 days of culturing period. The temperature and pH of the photobioreactor were recorded using the control panel and a portable pH meter (LAQUA B-712, Horiba, Moulton Park, United Kingdom). Outdoor temperature was manually recorded using Sheffield's daily weather forecast report. Light intensity was measured using a digital light meter (LX1330B, Dr. meter, China).

Throughout the 15-day experimental period, a 1 L sample was taken every day at 9 a.m. and the OD (λ = 595 nm) was measured to monitor the growth of the microalgae. A volume of 5 mL of culture was used for each analysis of DCW, proteins and chlorophylls, lipids, and EPA, with samples collected in three technical replicates for all analyses. After harvesting the cell pellets were centrifuged (SL16R, Thermo Fischer Scientific, United Kingdom) at 4415 ×*g* for 5 min, they were washed with phosphate-buffered saline and centrifuged again (11,337 ×*g* for 2 min) before storage at −20 °C. The supernatant was used for the nitrate and phosphate uptake assays.

2.3. Physiological and biochemical analysis

Cell pellets were freeze-dried for 24 h by using a freeze drier (Lyo-Quest, Telstar, United Kingdom), and the DCW was measured using a microbalance (CPA2P, Sartorius, OH, United States). Chlorophylls and proteins were quantified by using the spectrophotometric method in triplicate (Chen and Vaidyanathan, 2013). First, cell pellets were lysed using a cell disruptor (DISRUPTOR GENIE®, United States) with glass beads. Then, the samples were saponified by heating at 100 °C for 30 min (Digital Dry bath, Thermo Fisher Scientific, United Kingdom). An aliquot of 600 µL was used for protein assay, and the remaining sample was mixed with chloroform and methanol in a 2:1 ratio (v/v), vortexed for 2 min and centrifuged at 12,000 ×*g* for 2 min. The top aqueous phase was used for chlorophyll *a* assays. A volume of 500 µL of samples was aliquoted into a 1 mL (2 mm) quartz cuvette and measured by spectrophotometer at 416 nm and 453 nm. The equation (chlorophyll-*a* = 6.4 × A416–0.79 × A453) was used to calculate the chlorophyll-*a* as described by a previous study (Chen and Vaidyanathan, 2013). The protein assay was quantified using the microbiuret method and bovine serum albumin (BSA) as a standard curve (Itzhaki and Gill, 1964). In brief, 150 µL of copper sulphate (0.21 % $CuSO_4$*$5H_2O$ in 30 % NaOH) was added to 300 µL samples. 150 µL of 30 % NaOH was added to the other 300 µL samples for blank reference. The samples were vortexed for 5 min, and a spectrophotometer recorded the colour formation at 310 nm. The procedures for measuring the levels of nitrate (Collos et al., 1999) phosphate (Strickland and Parsons, 1972) in f/2 medium were modified from prior research conducted, respectively. The filtered supernatants from the collected samples were retained after passing through a 0.22 µm syringe filter (Millex, United Kingdom). The concentration of nitrate and phosphate was measured for each sampling day by calculating the absorbance values at 220 nm and 885 nm, respectively.

2.4. Fatty acids analysis

The FAME analysis method used in this study was adapted from (Griffiths et al., 2010) with some modifications. To summarize the procedure, 300 µL toluene and 300 µL sodium methoxide were added to a 2 mL Eppendorf tube containing wet microalgal biomass. After incubation at 80 °C for 20 min and cooling, 300 µL boron trifluoride was added, and the mixture was incubated again. The extracted solution was then transferred to a new Eppendorf tube containing water and hexane, and the upper organic layer was collected for further analysis. The extract was dried using inert nitrogen gas and stored at −20 °C until further use. For analysis, 35 µL of the FAME extract was transferred to a GC vial and analysed using a GC-FID system (Thermo Fisher Scientific, United Kingdom). The peak areas were integrated using a chromatography data system, and the amount of unknown components in the microalgal extract was then calculated in mg/g DCW. Standard 37 FAME was used for all 24 samples to ensure the system's accuracy. The identities of the peaks were established using an external 37 component mix of FAME standards (Supelco, USA), C16, C18, and C20:5 standards. The peak areas were integrated using a chromatography data system, Chromeleon 7 software (Thermo Fisher Scientific, United Kingdom).

2.5. Techno-economic assessment

The TEA was conducted by integrating the optimum EPA quantity into the developed TEA model by a previous study (Schade and Meier, 2021). Microalga oil economic data was selected as baseline data, where 42 g EPA/kg DCW and 13,225 kg/annum of microalga oil production were estimated (Table 1). In this study, the average optimum EPA quantities recorded for wild-type and M1 strains *N. oculata* from day 4 until day 7 were used for economic assessments.

The temperature and hours of daylight comparison between the location used for the model study, Halle, Germany, and this study based in Sheffield, United Kingdom, are shown in Table 2. The data comparison shows that the high-temperature average is within range for strains of *Nannochloropsis* culturing, and the hours of daylight are comparable, enabling the Schade and Meier (2021) model to be used for assessing the wild-type and M1 strains culturing in Sheffield, United Kingdom.

Table 1
Parameters and input of microalga biomass, lipid, and EPA production comparisons for baseline *Nannochloropsis* sp., wild-type, and M1 strains *N. oculata*. All other parameters and input are considered constant variables and similar to the baseline *Nannochloropsis* sp.

Parameter	Unit	Baseline *Nannochloropsis* sp.	Wild-type *N. oculata* (this study)	M1 strain *N. oculata* (this study)
Lipids	g/kg DCW	206	206	206
EPA	g/kg DCW	42	57.6	87.02
Total microalga cell yield	kg/1.2 ha/annum	64,200	64,200	64,200
Biomass residue	kg/1.2 ha/annum	50,917	50,917	50,917
Microalga oil	kg/1.2 ha/annum	13,225	13,225	13,225
Land	ha	1.2	1.2	1.2

Referring to the baseline data by Schade and Meier (2021), a new baseline was obtained for wild-type and M1 strains *N. oculata*, respectively. Then, there were four scenarios considered for the wild-type and M1 *N. oculata* strains, respectively. The first scenario considered a faster growth rate of 28.3 %, that was estimated by growth of wild-type and M1 strains in the laboratory setup. The faster growth rate indicates that each experiment could reach a higher EPA quantity. In the second scenario, the baseline study increased the culturing operations days to 80 % (292 days) instead of 50 % (183 days). The increase of working days to 80 % was considered in order to optimise the profits gained, hence shortening the payback period. The operational cost increased proportionally with the number of days. In the third scenario, the potential of the wild-type and M1 strains to produce 50 % higher biomass due to sunlight availability throughout the year in tropical countries such as Malaysia and Indonesia (Handara et al., 2016). These scenarios are crucial in influencing production costs (Chauton et al., 2015). The fourth scenario combines the changes made in all scenarios (Scenario 1, 2 and 3) to achieve an overall 'best-case' scenario (Leflay et al., 2020). Net present value (NPV) was calculated by referring to the equation:

$$NPV_n = \frac{NCF}{(1+d)^n},$$

Table 2
Average daily temperature and hours of daylight comparison between Halle, Germany and Sheffield, United Kingdom, referring to a forecast website (https://weatherspark.com/). The website uses the NASA climate model, Modern Era Retrospective-analysis for Research and Applications (MERRA-2, https://gmao.gsfc.nasa.gov/reanalysis/MERRA-2/).

Place	Conditions	June	July	August
Halle, Germany	High-temperature average (°C)	22	24	24
	Low-temperature average (°C)	12	14	14
	Hours of daylight (h)	16.6	16.1	14.5
Sheffield, United Kingdom	High-temperature average (°C)	18	20	20
	Low-temperature average (°C)	10	12	12
	Hours of daylight (h)	16.9	16.4	14.7

where NCF is the net cash flow of a time period n, and d is the nominal discount rate set at 12 % (Schade and Meier, 2021). Return on investment (ROI) was calculated by referring to the equation:

$$ROI = \sum_{3}^{n} \frac{NPV_n - C_{tot}}{C_{tot}},$$

where total costs (Ctot) represent the sum of payments assigned in the first and second years when all investment costs were paid (Schade and Meier, 2021).

3. Results and discussion

3.1. Physiological and biochemical analysis of wild-type and M1 *N. oculata* strains

On 27 July 2019, the M1 strain *N. oculata* experiment was conducted in a 300 L photobioreactor for a 15-day period. The growth started with a lag growth phase from day 0 until day 2 due to partly cloudy weather with a temperature range of 16–17 °C, and limited light intensities as shown in Figs. 1 and 2. When the weather changed from cloudy to sunny on day 3, the growth rate of microalgae cells increased sharply (to 0.38 per day) from day 4 to day 8. This implied light limitation during the initial lag phase, as increased light enabled higher photosynthetic rates (Stunda-Zujeva et al., 2018). These observations were similar to a previous outdoor pilot scale study, where cloudy weather conditions were less favourable for microalgae growth (Kumar et al., 2023). The cells continued to grow at a slower rate (0.12 per day) from day 9 to day 12, and the exponential growth phase ended on day 13. Meanwhile, a slower growth rate was recorded from day 9 to 12, which was most likely due to nitrate-depleted conditions as shown in Fig. 3 (b). Nitrogen depletion is a common reason for microalgae to enter the stationary phase of growth (Zhou et al., 2023). The highest temperatures recorded during the experiment were on days 3, 8, and 9, with 23, 25, and 24 °C, respectively. This may be due to increased sunlight hours during this time increasing the temperature inside the polycarbonate housing. The pilot-scale photobioreactor was intentionally performed with limited control of conditions that can impact on microalgae growth, and therefore relied on environmental weather conditions. However, the unpredictable weather conditions didn't significantly affect microalga cell growth. The average temperature throughout the experiment was 19.9 °C, and the average light intensity was 969.6 μmol m^{-2} s^{-1}, with a 15:53-h/8.47-h (light/dark) cycle.

The light intensity is shown in Fig. 2 and represents measurements during the sampling time from 9 a.m. until 10 a.m. only, and hence the light intensity is expected to be higher during partly cloudy days in the afternoon than cloudy days. A higher concentration of 4.5 % CO_2 (v/v) was needed to regulate the pH over 15 days of the culturing period for the wild-type *N. oculata*, compared to 4 % CO_2 (v/v) for the M1 strain. It is not immediately clear why there was a difference. A similar strain showed 4 % CO_2 led to the most increased CO_2 fixation in wild-type *N. gaditana*, that were cultured in an 18 L photobioreactor (Adamczyk et al., 2016). However, this can change based on the cultivation conditions as another study using *N. oculata* found 8 % CO_2 was the optimum concentration for growth in a 1.8 L photobioreactor (Razzak et al., 2015). Higher concentrations of CO_2 are often detrimental to growth rates, for example, 10 % and higher was reported to reduce the growth of *Nannochloropsis* sp. (Lestari et al., 2019). It has been reported that maintaining the *N. gaditana* culture at pH 8 allows the optimum CO_2 conversion in biomass (Moraes et al., 2020), perhaps due to reducing stress as pH fluctuations are minimised. Providing the optimal amount of CO_2 will increase the carboxylation activity of ribulose-1,5-biphosphate carboxylase/oxygenase (RubisCO), hence increasing photosynthesis rates. However, excess CO_2 concentrations negatively affect extracellular carbonic anhydrase activity and impede microalgae cell growth (Kandasamy et al., 2021). Hence, high CO_2 concentrations,

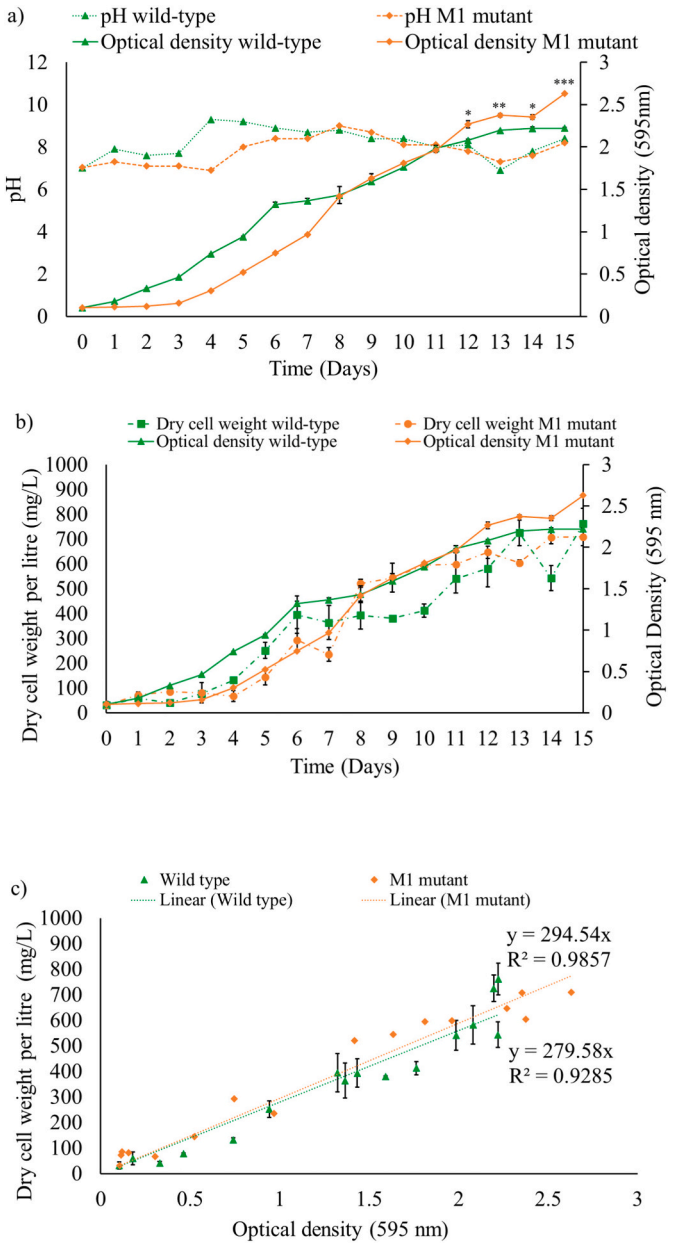

Fig. 1. Growth profiles for wild-type and M1 strain *N. oculata* cultivated in an outdoor 300 L Photobioreactor supplied with CO_2. a) Optical density at 595 nm and pH profiles, b) and c) dry cell weight and optical density at 595 nm correlation.

for example, over 10 %, can impede photosystem efficiency, hence reducing microalgae cell growth (Varshney et al., 2020). Further investigation is needed to reveal the specific effects of CO_2 concentrations on RubisCO, extracellular carbonic anhydrase activity and growth development in the *N. oculata* M1 strain.

The OD profile was directly proportional to chlorophyll-*a*, as expected. Chlorophyll-*a* showed a rapid increase from day 4 to day 8, followed by moderate increases until day 14, and decreased on day 15, as depicted in Fig. 3 (a). The highest chlorophyll-*a* level was observed on day 14 at 3.94 μg/mL for the M1 *N. oculata* strain. The chlorophyll-*a* results in this study are consistent with the other studies for *N. gaditana* and *Nannochloropsis* sp. that ranged around 2 to 3 μg/mL (Fakhri et al., 2017; Janssen et al., 2018). However, cell densities and therefore chlorophyll-*a* content can be increased by using novel cultivation systems. For example, *N. oculata* cultured in a novel lab-scale open raceway

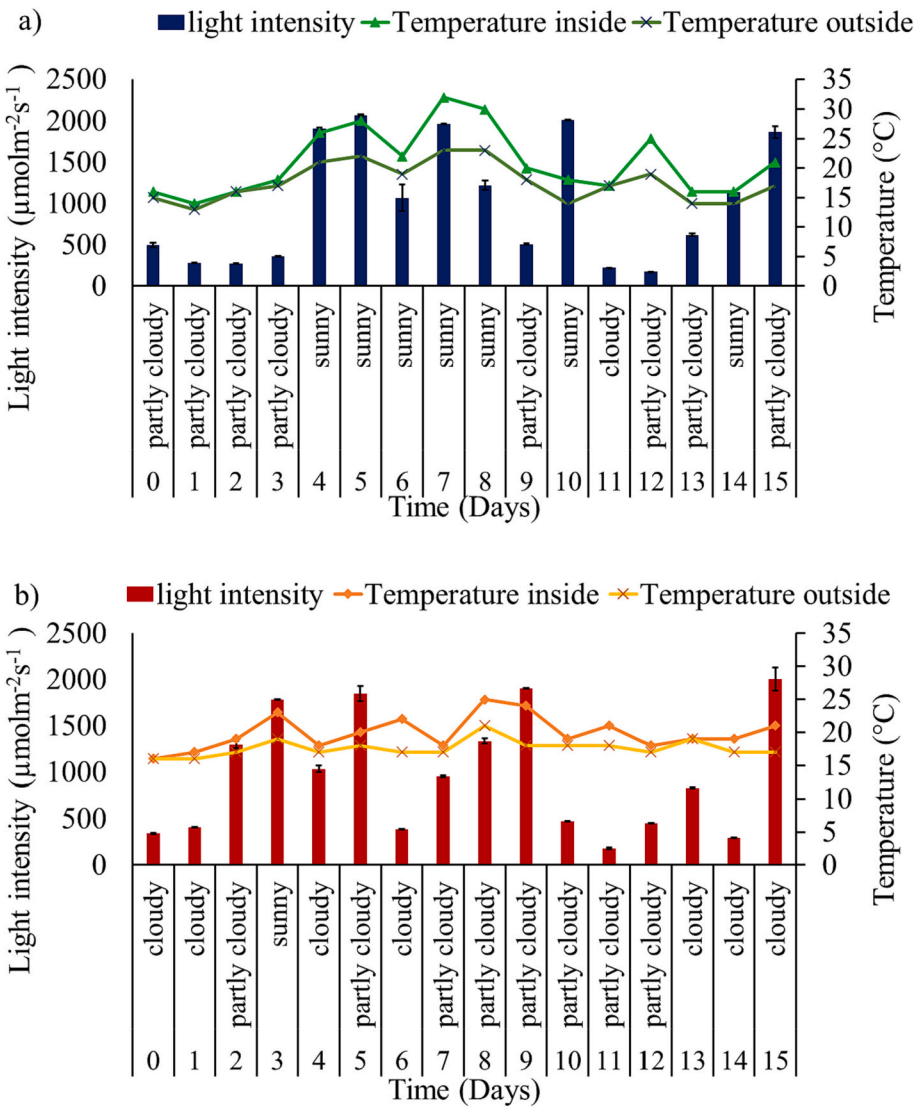

Fig. 2. Temperature and weather profiles throughout 15 days experimental period: a) wild-type supplied with CO_2, b) M1 strain *N. oculata* supplied with CO_2. Cloud levels are described at time point of sampling only (9 am – 10 am).

pond with planar waveguide modules recorded a higher chlorophyll-*a* (15.36 μg/mL) (Sun et al., 2018). Similarly, *N. oceanica* was cultured in a vertical column photobioreactor designed to apply direct current to cells, recorded around 13 μg/mL chlorophyll-*a* (Cheng et al., 2022).

Nitrate was fully utilized on day 10, whereas phosphate was rapidly consumed on day 3, as shown in Fig. 3 (b) and (c), respectively. The phosphate uptake rate was 28.56 μM/day from day 3 to day 4. The M1 mutant's protein content was highest from day 8 to day 12, ranging from 0.22 to 0.38 mg/mL, as illustrated in Fig. 3 (d).

Figs. 4(b) and 5(b) depict the FA contents of M1 strain *N. oculata* that was supplied with CO_2. From day 0 to day 3, the percentage of C16:0 and C16:1 was approximately 24–30 %. However, on day 4, when growth was optimal, there was a significant decrease in the percentage of C16:0 and C16:1 with 13.28 % and 18.85 %, respectively. During this time, EPA levels increased and reached its peak from day 4 to day 7. On day 5, the highest percentage of EPA (42.77 %) of TFA was recorded. The EPA to C16:0 ratio was 2.85, 2.49, and 1.43 on days 4, 5 and 6, respectively. From day 7 onwards, the ratio fell below 1, indicating that C16:0 was again the dominant FA in the cells. From day 7 to day 15, C16:0 and C16:1 again became the dominant FA and reached their highest percentage on day 15 (35–36 %). The higher EPA percentage during the exponential phase is mainly synthesized in the polar lipids, while the EPA is translocated to neutral lipids when the nutrients become depleted during stationary phase (Janssen et al., 2019).

On days 4, 5 and 6, EPA levels were higher than C16:0 and C16:1. The highest amount of EPA was recorded on day 7 (129.87 mg/g DCW) with an EPA to C16:0 ratio of 0.73. Interestingly, from day 8 to day 15, EPA levels remained significantly high, ranging from 41 to 69.8 mg/g DCW, while C16:0 and C16:1 levels were highest on day 15 with 215.20 and 281.74 mg/g, respectively.

The wild-type *N. oculata* experiment was conducted for 15 days starting from August 18, 2019. During the initial six days, the microalgae exhibited an exponential growth curve with an average rate of 0.42 per day. However, the growth rate decreased to 0.07 per day from day 6 until the end of the late exponential growth phase on day 13. The decrease in growth rate is expected since the phosphate was consumed in 4 days and nitrate concentration was reduced around 50 % after day 6. A similar growth trend is observed for other *Nannochloropsis* species (Alami et al., 2021). The experiment was conducted at an average temperature of 20.9 °C and 1009.9 μmol m^{-2} s^{-1} with a 14:07-h/9.93-h (light/dark) cycle, as depicted in Fig. 2 (a).

Fig. 3 (a) illustrates that the quantity of chlorophyll-*a* increased rapidly until day 5, moderately increased until day 8, and then gradually declined towards the end of the 15-day experimental period. Day 8 had

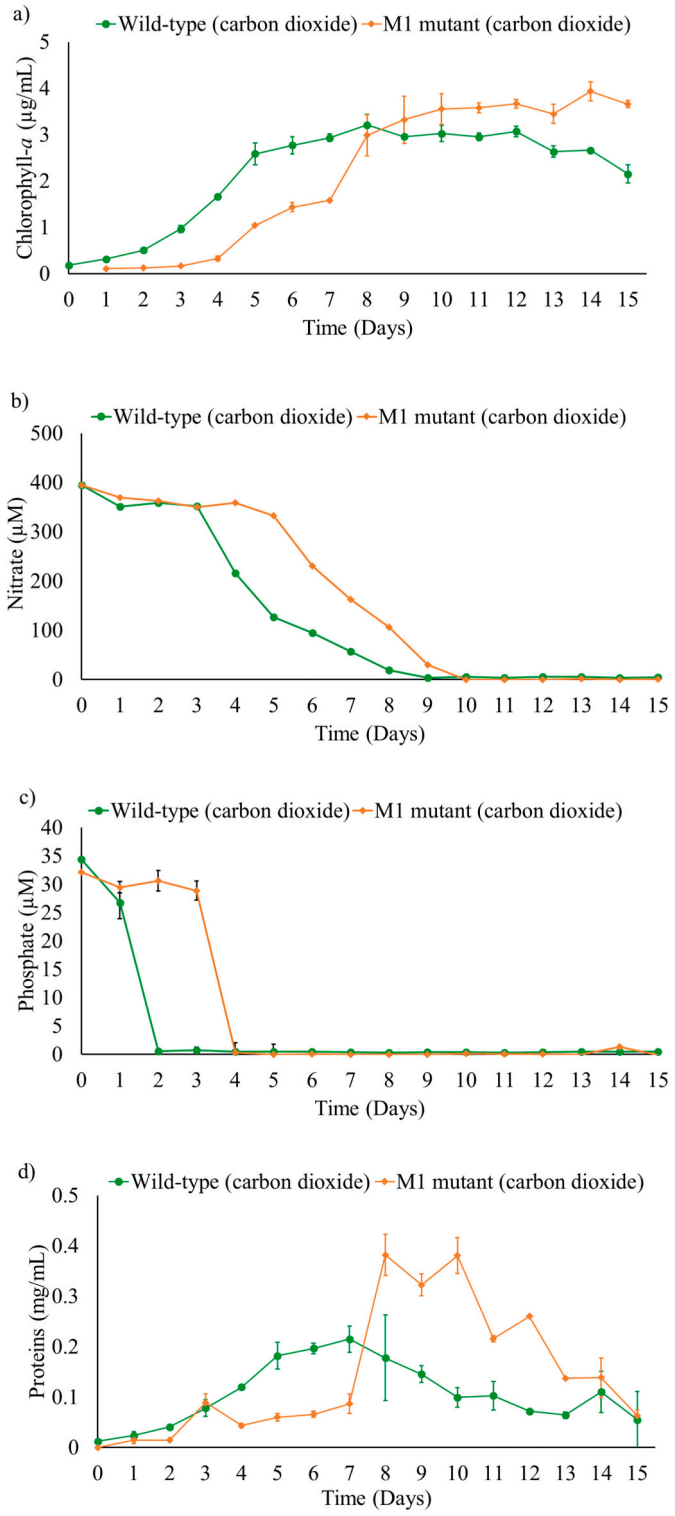

Fig. 3. Profiles for wild-type and M1 strains of *N. oculata* cultivated in an outdoor 300 L pilot-scale photobioreactor supplied with CO_2. a) Chlorophyll-a, b) nitrate uptake, c) phosphate uptake, and d) protein quantity profiles. Mean ± standard deviation is shown (n = 3) for each day.

the highest chlorophyll-*a* quantity, which was 3.2 µg/mL. Although the wild-type strain showed rapid growth progress, the average chlorophyll-*a* level was higher in the M1 strain. The fast growth of the microalgae indicated a faster nitrate uptake that was completely consumed by day 9, one day earlier than the M1 strain, as depicted in Fig. 3 (b). The nitrate uptake rate from day 0 until day 7 was 48.27 µM/day and 33.11 µM/day for wild-type and M1 strains *N. oculata*, respectively. The adverse weather condition on the initial day 1 and 2 affected the initial growth and nitrate uptake rate of the M1 strain. The wild-type's rapid growth was also demonstrated by a fast phosphate uptake rate that was completely consumed by day 2, as illustrated in Fig. 3 (c). The rapid phosphate uptake correlates to fast microalgae growth, as the macronutrient phosphorus is an essential component of microalgae. Microalgae can rapidly consume phosphate when in replete conditions, maintaining growth when concentrations in the media are depleted (Manisali et al., 2019). Fig. 3 (d) shows that the protein quantity gradually increased from day 0 until day 7, reached the highest point of 0.22 mg/mL, and then gradually decreased from day 8 until day 15. On average, the protein quantity of the wild-type *N. oculata* was lower than that of the M1 strain.

High chlorophyll-*a* content in M1 strain was in line with findings in our previous study (Wan Razali et al., 2022), indicating that the light-harvesting capacity in the M1 strain is higher than the wild-type strain, hence enhancing chlorophyll-*a* and EPA production. In addition, the pathway changes in the M1 strain could promote higher chlorophyll synthesis, hence, increasing the EPA content, that is mainly synthesized in membrane polar lipids (Janssen et al., 2019). A faster nitrate uptake rate during optimum growth conditions could also contribute to a higher chlorophyll-*a* and protein content in the M1 strain as indicated in a previous study (Hernández-Sandoval et al., 2022). In contrast, nitrate limited conditions is a known trigger for neutral lipid synthesis in many oleaginous microalgae (Burch and Franz, 2016; Remmers et al., 2017; Tran et al., 2016) The decrease in protein content resulting from nitrogen deprivation is consistent with a previous study (Sui et al., 2019). In another study, the neutral lipids decreased while the protein increased when nitrate was replenished in a *Nannochloropsis* sp. culture (Li et al., 2020). Phosphate was rapidly consumed for both wild-type and M1 strains, indicating that a higher phosphate concentrations or regular dosing could be employed in the future. A previous study recorded up to 20.05 mg/g/day phosphate consumption rate in *N. salina* (Sforza et al., 2018), and 2 g/L phosphate showed the highest OD in *N. oculata* (Mahat et al., 2015). In addition, an optimised N:P ratio concentration could be prepared as a 20 N:P ratio showed the highest EPA percentage in *N. oculata* (Rasdi and Qin, 2015).

Figs. 4(a) and 5(a) display the FA contents of wild-type *N. oculata* supplied with CO_2. The percentage of FA showed 42.68 % and 37.55 % EPA on days 3 and 4, respectively. The EPA to C16:0 ratio was 2.23 and 1.47 on days 3 and 4, respectively, while from day 5 until day 15, the ratio dropped below 1, indicating that C16:0 dominated the microalgae cells. Towards the end of the culturing period, C16:0 and C16:1 showed an average of 35–36 %. Although the EPA percentage was highest on days 3 and 4, the EPA quantity recorded 39.66 mg/g DCW and 66.26 mg/g DCW on those days, respectively. On day 10, the highest EPA was recorded at 75.43 mg/g DCW with an EPA to C16:0 ratio of 0.58.

TFA comparison for wild-type and M1 strains *N. oculata* is shown in Table 3. The M1 strain indicated a higher TFA than the wild-type strain. The TFA could reach around 270 to 300 mg/g DCW in wild-type *N. oculata* cultured under nitrate and phosphate limitation for 5 days of the culturing period (Gong et al., 2013).

The biochemical results were in agreement with an enhanced EPA quantity in M1 *N. oculata* (129.87 mg/g DCW), while the wild-type strain EPA quantity (75.43 mg/g DCW) was relatively higher than quantified in similar studies (Camacho-Rodríguez et al., 2014; Chen et al., 2018; Chen et al., 2015; Chen et al., 2013; Hulatt et al., 2017; Willette et al., 2018). However, despite a lower absolute EPA quantity, the EPA percentage of TFA reached 42.68 % in the wild-type strain, a comparable result to the EPA percentage in M1 strain, which recorded 42.77 %. The reason for the higher EPA content recorded in the wild-type was not clear, although conditions in the pilot-scale photobioreactor design could have contributed. A high ratio of EPA to C16:0 is a useful indicator for identifying the ideal time for harvesting cells whilst maximizing the EPA concentration. The M1 strain had a higher

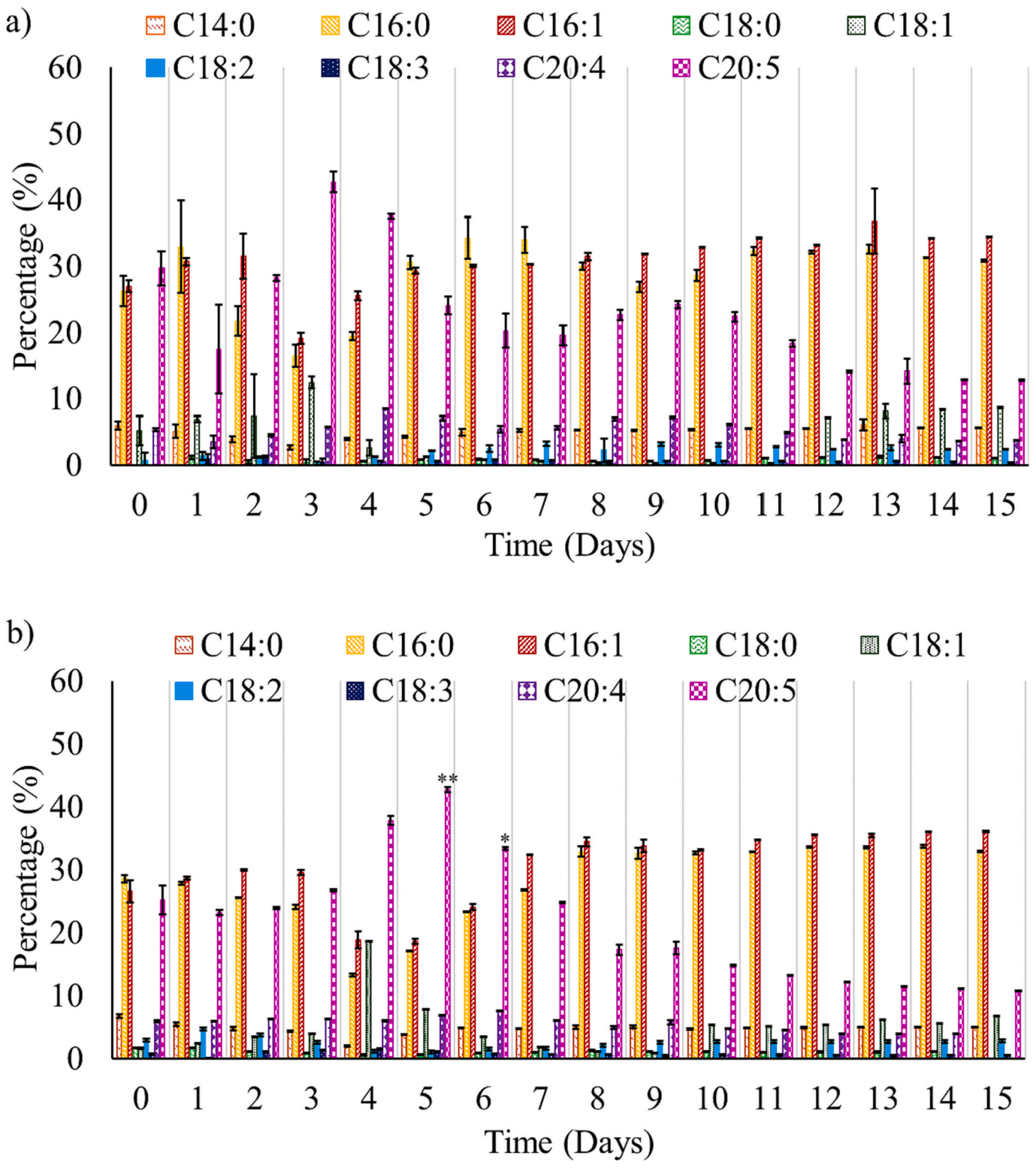

Fig. 4. Percentages of main fatty acid profiles: a) wild-type, and b) M1 strain *N. oculata* supplied with 4.5 and 4 % CO_2 (v/v), respectively. The data show the mean value and standard deviation of three technical replicate samples. The significant differences, determined by Student's *t*-test, are indicated by asterisks (*$p < 0.05$, **$p < 0.01$, ***$p < 0.001$).

overall oil content than the wild-type strain, due to changes in FA synthesis and degradation pathways as described previously (Wan Razali et al., 2022).

3.2. Techno-economic assessment results

The TEA analysis was conducted by integrating the optimum EPA quantity data for wild-type and M1 *N. oculata* strains in this study into a TEA model described in a previous study (Schade and Meier, 2021). The system referred to an outdoor 628 m^3 tubular photobioreactor located in

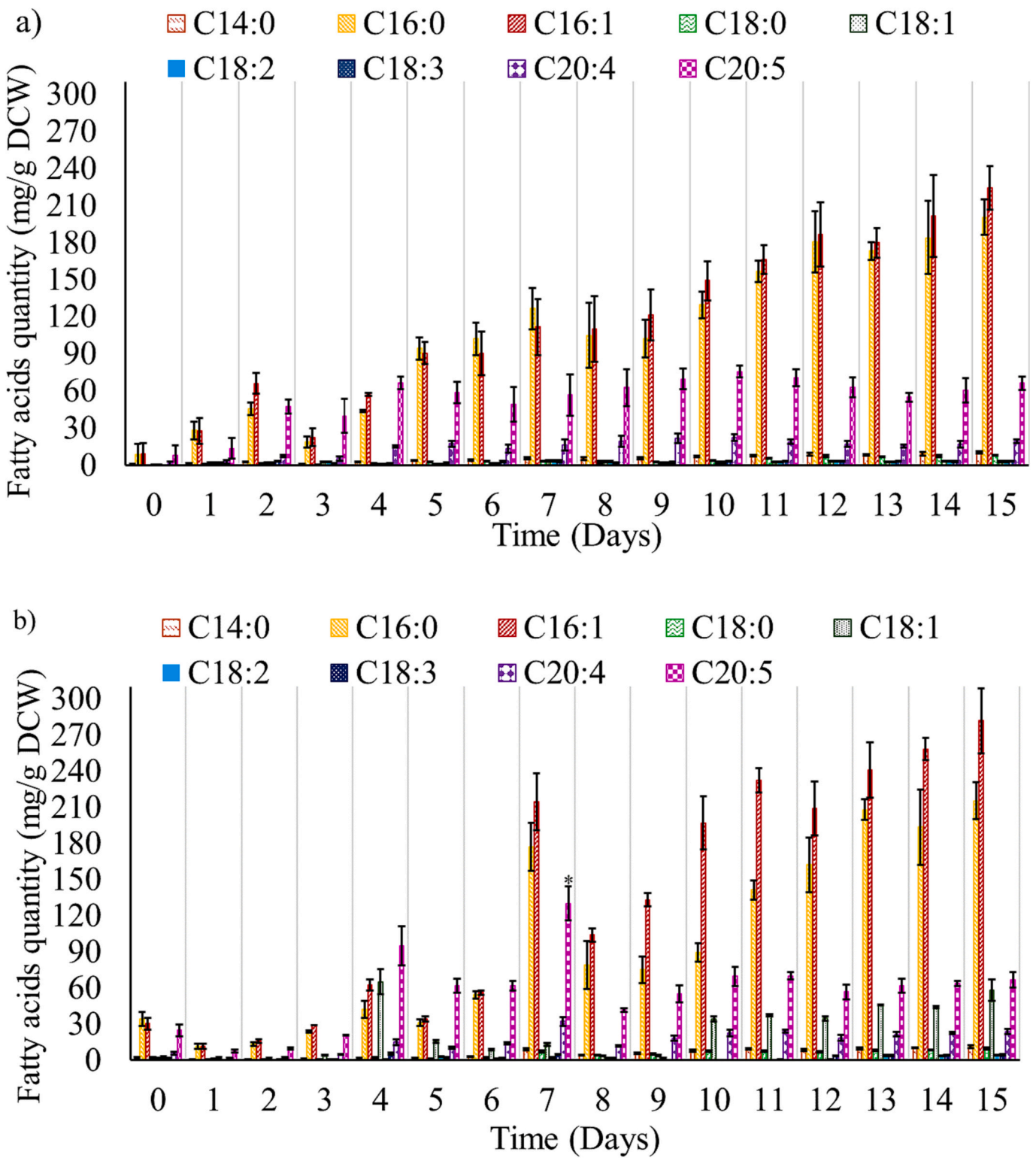

Fig. 5. Quantification of main fatty acid profiles. a) Wild-type and b) M1 strain *N. oculata* supplied with 4.5 and 4 % CO_2 (v/v), respectively. The data show the mean value and standard deviation of three technical replicate samples. Asterisks indicate the significant differences determined by Student's t-test (*$p < 0.05$, **$p < 0.01$, ***$p < 0.001$).

Halle/Saale, Germany (Schade and Meier, 2021). All measured parameters are assumed suitable for growing strains at the optimal growth rate. In the TEA analysis, four possible scenarios were evaluated. The cost projection was calculated by referring to the baseline data (Schade and Meier, 2021) as shown in Tables 4 and 5. The scenarios studied the economic impact of M1 strain EPA quantity (87.02 g/kg DCW) when the microalga oil production was higher than the baseline data. In the baseline scenario, a weight of 64,200 kg of *Nannochloropsis* sp. biomass was produced in one year, and 13,225 kg accounted for total lipids or microalga oil. The other valuable side product was biomass residue left after the microalga oil was extracted. The yearly production of 50,917 kg/year was accounted for biomass residue; the by-product after the

Table 3
TFA profiles (mg/g DCW) for wild-type and M1 strain *N. oculata*. The data show the mean value of three technical replicate samples.

Days	Wild-type (4.5 % CO_2) (v/v)	Standard deviation (±)	M1-strain (4 % CO_2) (v/v)	Standard deviation (±)
0	27.59	5.58	104.85	18.48
1	77.92	32.07	36.66	6.21
2	174.26	28.27	45.04	4.48
3	92.36	33.18	86.27	1.02
4	188.14	9.80	289.21	41.92
5	270.22	29.31	160.69	13.11
6	266.28	48.87	203.06	11.16
7	328.55	45.62	590.10	65.03
8	310.83	74.26	250.86	24.98
9	327.46	48.90	296.73	19.46
10	393.60	33.60	428.63	37.89
11	432.93	30.71	522.43	19.52
12	472.07	70.64	499.76	55.99
13	446.64	28.23	602.58	38.63
14	487.95	86.98	607.80	45.84
15	536.94	45.20	674.45	54.82

microalga oil was removed. The biomass residue could also be used as animal and fish feed. The price of fish feed was estimated at €1091 or equivalent to £938.26 per tonne (Shield and Lupatsch, 2012). The conversion rate from euro to pound when this study was conducted was 1 euro equals 0.86 pounds. The NPV and ROI calculations are shown in the supplementary Table S1 until S11.

NPV and ROI are two financial metrics that are used to evaluate the significance indicators for the economic potential of the studied scenarios. Table 6 shows 10-year comparison of NPV and ROI for this study. The ROI for the M1 strain was expected at 110.99 % after 10 years of operations. On the contrary, *Nannochloropsis* sp. and wild-type *N. oculata* have ROI −0.10 % and 39.68 %, respectively, after 10 years of operations, which are unprofitable. Having 28.3 % growth faster for wild-type showed an increase of ROI 124.63 % after 10 years. Having 80 % of running of total days per year has reduced the ROI to 94.09 %, while, the accumulation of 50 % microalga biomass cultured in tropical countries has increased the ROI to 109.52 % after 10 years. Combining all the scenarios, higher growth, 80 % operational days per year and the setup in tropical countries has significantly increased the ROI to 368.20 % after 10 years.

A higher EPA quantity in the M1 strain contributed to 110.99 % ROI after 10 years. A faster growth (28.3 %), 80 % operational days per year, and 50 % biomass increase for the setup in tropical countries recorded ROI at 239.30 %, 193.18 % and 216.49 %, respectively. Combine scenarios showed 607.22 % ROI after 10 years, indicating a profitable business.

EPA quantity per cell in the M1 strain was significantly higher compared to the EPA quantity reported in other studies (Camacho-Rodríguez et al., 2014; Chen et al., 2018; Chen et al., 2015; Chen et al., 2013; Hulatt et al., 2017; Willette et al., 2018). 110.99 % ROI and £8,129,226,70 NPV after 10 years indicate 87.02 mg/g DCW EPA quantity has doubled the initial investment. The results demonstrated that the M1 strain reaches the breakeven point after 10 years and gains profits in a few more years. The break-even point is when the investment cost of developing the microalga plant equals the revenue from sales, hence starting to generate a profit (Mohammady et al., 2022). The baseline scenario showed that at least 10 years and 6 months are required for a plant to show a positive ROI from selling biomass, while at least 24 years is needed for microalga oil of wild-type *Nannochloropsis* sp. industry to portray a positive ROI (Schade and Meier, 2021). Therefore, further strategies must be implemented to gain profits in a shorter period.

In this study, wild-type *N. oculata* reached a break-even point in 22 years while baseline data indicated *Nannochloropsis* sp. microalga oil could never make a profit. On the contrary, a higher EPA quantity in the M1 strain indicated a break-even point is reachable in 10 years. A higher growth rate (28.3 %) for wild-type showed a faster break-even point in 9 years with NPV achieving £9,128,236.14 after 10 years. 80 % more operational days per year and 50 % more biomass in tropical countries setup showed NPV of £7,913,862.55 and £8,021,781.11, respectively.

The increase in the M1 strain growth rate could shorten the break-

Table 4
Parameters and input for four possible scenarios to be applied to wild-type *N. oculata* to increase microalga oil production productivity. All other parameters and information are considered constant variables similar to the baseline *Nannochloropsis* sp. (Schade and Meier, 2021).

Parameter	Unit	WT *N. oculata* (grow 28.3 % faster)	WT *N. oculata* (292 day per year)	WT *N. oculata* (tropical country)	WT *N. oculata* (combined scenarios)
Lipids	g/kg DCW	206	206	206	206
EPA	g/kg DCW	57.61	57.61	57.61	57.61
Total microalga cell yield	kg/1.2 ha/annum	103,242.20	102,439.34	96,292.72	247,106.8
Biomass residue	kg/1.2 ha/annum	81,881	81,244.61	76,375.5	195,980.4
Microalga oil	kg/1.2 ha/annum	21,267.79	21,102.19	19,837.5	50,903.24
Land	ha	1.2	1.2	1.2	1.2

Table 5
Parameters and input for four possible scenarios to be applied to M1 strain *N. oculata* to increase microalga oil production productivity. All other parameters and information are considered constant variables similar to the baseline *Nannochloropsis* sp.(Schade and Meier, 2021).

Parameter	Unit	M1 strain *N. oculata* (grow 28.3 % faster)	M1 strain *N. oculata* (292 day per year)	M1 strain *N. oculata* (tropical country)	M1 strain *N. oculata* (combined scenarios)
Lipids	g/kg DCW	206	206	206	206
EPA	g/kg DCW	87.02	87.02	87.02	87.02
Total microalga cell yield	kg/1.2 ha/annum	103,242.20	102,439.34	96,292.72	247,106.8
Biomass residue	kg/1.2 ha/annum	81,881	81,244.61	76,375.5	195,980.4
Microalga oil	kg/1.2 ha/annum	21,267.79	21,102.19	19,837.5	50,903.24
Land	ha	1.2	1.2	1.2	1.2

Table 6
Net present value (NPV) and return of investment (ROI) comparisons for 10 years timeline.

	Case study	Net present value (NPV) (£) after 10 years	Return of investment (ROI) after 10 years
1	Baseline *Nannochloropsis* sp.	-7354.08	-0.10 %
2	Wild-type *N. oculata*	2,906,431.17	39.68 %
3	Wild-type *N. oculata* (28.3 % growth faster)	9,128,236.14	124.63 %
4	Wild-type *N. oculata* increased to 80 % of running of total days/year	7,913,862.55	94.09 %
5	Wild-type *N. oculata* (accumulates 50 % more biomass in tropical countries)	8,021,781.11	109.52 %
6	Wild-type combine Scenario (3, 4, & 5)	32,053,860.19	368.20 %
7	M1 strain *N. oculata*	8,129,226.70	110.99 %
8	M1 strain *N. oculata* (28.3 % growth faster)	17,527,277.25	239.30 %
9	M1 strain *N. oculata* increased to 80 % of running of total days/year	16,247,505.17	193.18 %
10	M1 strain *N. oculata* (accumulates 50 % more biomass in tropical countries)	15,855,974.41	216.49 %
11	M1 strain combine Scenario (8, 9, & 10)	52,156,484.46	607.22 %

even point to the end of 6 years, as the NPV achieves £17,527,277.25 after 10 years. Increasing the operation period to 292 days/year also could shorten the break-even point to an early 7 years, as the NPV achieves £16,247,505.17 after 10 years. Culturing the M1 strain in tropical countries showed NPV of £15,855,974.41 and break-even period of 7 years. Tropical countries with consistent light intensities and temperatures could be the ideal place to culture microalgae. For example, in tropical country Malaysia, at a lower altitude place such as Kuala Lumpur, the daily temperature is around 26–28 °C (Rahman, 2018; Tang, 2019). On the other hand, in a high-altitude place like Cameron Highland, the average daily temperature ranges from 15 to 22 °C, which could be an ideal place for culturing and maximizing the EPA synthesis (Tan et al., 2021). The 'best case' scenario shows the highest ROI and NPV as expected, with a break-even point as early as year 4 for the M1 strain and gaining profit afterwards. After 32 years, the ROI is expected at 919.03 %, about nine times of initial investments with an NPV of £98,727,632.36. A similar result showed for the 'best case' scenario for the wild-type *N. oculata* with 5 years of break-even, 574.63 % ROI and £62,419,795.68 after 32 years.

Overall, the M1 mutant shows significant promise in our TEA using data extrapolated from the experimental runs. A further advantage is the strain is not classified as genetically modified minimising regulatory issues. Challenges include unpredictable productivity rates in outdoor systems with minimal cultivation control.

4. Conclusion

The physiological and biochemical results obtained from the 300 L pilot-sized outdoor photobioreactor demonstrated that it was appropriate for cultivation of both the wild-type and M1 strains of *N. oculata*. The exponential growth phase indicated the highest EPA quantity for both strains. However, the M1 strain indicated capabilities of producing higher amounts of EPA in an outdoor pilot-scale system. For TEA evaluation, the average EPA quantity in the exponential growth phase was integrated into a developed TEA model and evaluated to determine whether the enhanced EPA-based project is economically feasible. In conclusion, wild-type *N. oculata* achieves an upgrade in economic conditions under the improved scenarios one to three. The M1 strain characteristics imply the ability to overcome the high overall processing costs, while the improved scenarios for the M1 strain demonstrated further financial advantages in overcoming the high capital costs that currently exist within the microalgae industry.

CRediT authorship contribution statement

Wan Aizuddin Wan Razali:	1) Planned and Conducted experiments 2) Writing-original draft, review and editing manuscript
Jagroop Pandhal:	1) Planned the experiments 2) Writing, review and editing manuscript

Declaration of competing interest

The authors declare the following financial interests/personal relationships which may be considered as potential competing interests: Wan Aizuddin Wan Razali reports financial support was provided by Ministry of Higher Education Malaysia. Wan Aizuddin Wan Razali reports financial support was provided by Universiti Malaysia Terengganu. Jagroop Pandhal reports financial support was provided by Natural Environment Research Council.

Data availability

Data will be made available on request.

Acknowledgements

The authors would like to thank the Ministry of Higher Education Malaysia, and Universiti Malaysia Terengganu for funding this project. We also acknowledge funding from the Natural Environment Research Council (NE/PO16820/1).

Appendix A. Supplementary data

Supplementary data to this article can be found online at https://doi.org/10.1016/j.biteb.2023.101682.

References

Acién, F.G., Molina, E., Reis, A., Torzillo, G., Zittelli, G.C., Sepúlveda, C., Masojídek, J., 2017. Photobioreactors for the production of microalgae. In: Microalgae-based Biofuels and Bioproducts: From Feedstock Cultivation to End-products. Elsevier Inc., pp. 1–44. https://doi.org/10.1016/B978-0-08-101023-5.00001-7

Adamczyk, M., Lasek, J., Skawińska, A., 2016. CO2 biofixation and growth kinetics of Chlorella vulgaris and Nannochloropsis gaditana. Appl. Biochem. Biotechnol. 179, 1248–1261. https://doi.org/10.1007/s12010-016-2062-3.

Alami, A.H., Tawalbeh, M., Alasad, S., Ali, M., Alshamsi, M., Aljaghoub, H., 2021. Cultivation of Nannochloropsis algae for simultaneous biomass applications and carbon dioxide capture. Energy Sources A: Recovery Util. Environ. Eff. https://doi.org/10.1080/15567036.2021.1933267.

Barros de Medeiros, V.P., da Costa, W.K.A., da Silva, R.T., Pimentel, T.C., Magnani, M., 2022. Microalgae as source of functional ingredients in new-generation foods: challenges, technological effects, biological activity, and regulatory issues. Crit. Rev. Food Sci. Nutr. https://doi.org/10.1080/10408398.2021.1879729.

Burch, A.R., Franz, A.K., 2016. Combined nitrogen limitation and hydrogen peroxide treatment enhances neutral lipid accumulation in the marine diatom Phaeodactylum tricornutum. Bioresour. Technol. 219, 559–565. https://doi.org/10.1016/j.biortech.2016.08.010.

Camacho-Rodríguez, J., González-Céspedes, A.M., Cerón-García, M.C., Fernández-Sevilla, J.M., Acién-Fernández, F.G., Molina-Grima, E., 2014. A quantitative study of eicosapentaenoic acid (EPA) production by Nannochloropsis gaditana for aquaculture as a function of dilution rate, temperature and average irradiance. Appl. Microbiol. Biotechnol. 98, 2429–2440. https://doi.org/10.1007/s00253-013-5413-9.

Cecchin, M., Cazzaniga, S., Martini, F., Paltrinieri, S., Bossi, S., Maffei, M.E., Ballottari, M., 2022. Astaxanthin and eicosapentaenoic acid production by S4, a new mutant strain of Nannochloropsis gaditana. Microb. Cell Factories 21. https://doi.org/10.1186/s12934-022-01847-9.

Chauton, M.S., Reitan, K.I., Norsker, N.H., Tveterås, R., Kleivdal, H.T., 2015. A techno-economic analysis of industrial production of marine microalgae as a source of EPA

and DHA-rich raw material for aquafeed: research challenges and possibilities. Aquaculture 436, 95–103. https://doi.org/10.1016/j.aquaculture.2014.10.038.
Chen, Y., Vaidyanathan, S., 2013. Simultaneous assay of pigments, carbohydrates, proteins and lipids in microalgae. Anal. Chim. Acta 776, 31–40. https://doi.org/10.1016/j.aca.2013.03.005.
Chen, C.Y., Chen, Y.C., Huang, H.C., Huang, C.C., Lee, W.L., Chang, J.S., 2013. Engineering strategies for enhancing the production of eicosapentaenoic acid (EPA) from an isolated microalga Nannochloropsis oceanica CY2. Bioresour. Technol. 147, 160–167. https://doi.org/10.1016/j.biortech.2013.08.051.
Chen, C.Y., Chen, Y.C., Huang, H.C., Ho, S.H., Chang, J.S., 2015. Enhancing the production of eicosapentaenoic acid (EPA) from Nannochloropsis oceanica CY2 using innovative photobioreactors with optimal light source arrangements. Bioresour. Technol. 191, 407–413. https://doi.org/10.1016/j.biortech.2015.03.001.
Chen, C.Y., Nagarajan, D., Cheah, W.Y., 2018. Eicosapentaenoic acid production from Nannochloropsis oceanica CY2 using deep sea water in outdoor plastic-bag type photobioreactors. Bioresour. Technol. 253, 1–7. https://doi.org/10.1016/j.biortech.2017.12.102.
Cheng, J., Xin, K., Wang, Z., Zhu, Y., Xia, R., Yang, W., Liu, J., 2022. Improving biomass growth of Nannochloropsis oceanica with electrical treatment. J. CO2 Util. 58 https://doi.org/10.1016/j.jcou.2022.101923.
Collos, Y., Mornet, F., Sciandra, A., Waser, N., Larson, A., Harrison, P.J., 1999. An optical method for the rapid measurement of micromolar concentrations of nitrate in marine phytoplankton cultures. J. Appl. Phycol. 11, 179–184.
Cunha, P., Pereira, H., Costa, M., Pereira, J., Silva, J.T., Fernandes, N., Varela, J., Silva, J., Simões, M., 2020. Nannochloropsis oceanica cultivation in pilot-scale raceway ponds-from design to cultivation. Appl. Sci. 10 https://doi.org/10.3390/app10051725.
Fakhri, M., Arifin, N.B., Yuniarti, A., Hariati, A.M., 2017. The influence of salinity on the growth and chlorophyll content of Nannochloropsis sp. BJ17. Nat. Environ. Pollut. Technol. 16, 209–212.
Gammone, M.A., Riccioni, G., Parrinello, G., D'orazio, N., 2019. Omega-3 polyunsaturated fatty acids: Benefits and endpoints in sport. Nutrients. https://doi.org/10.3390/nu11010046.
Ghosh, S., Sarkar, T., Pati, S., Kari, Z.A., Edinur, H.A., Chakraborty, R., 2022. Novel bioactive compounds from marine sources as a tool for functional food development. Front. Mar. Sci. https://doi.org/10.3389/fmars.2022.832957.
Gong, Y., Guo, X., Wan, X., Liang, Z., Jiang, M., 2013. Triacylglycerol accumulation and change in fatty acid content of four marine oleaginous microalgae under nutrient limitation and at different culture ages. J. Basic Microbiol. 53, 29–36. https://doi.org/10.1002/jobm.201100487.
Griffiths, M.J., Van Hille, R.P., Harrison, S.T.L., 2010. Selection of direct transesterification as the preferred method for assay of fatty acid content of microalgae. Lipids 45, 1053–1060. https://doi.org/10.1007/s11745-010-3468-2.
Handara, V.A., Illya, G., Tippabhotla, S.K., Shivakumar, R., Budiman, A.S., 2016. Center for solar photovoltaics (CPV) at Surya University: novel and innovative solar photovoltaics system designs for tropical and near-ocean regions (an overview and research directions). In: Procedia Engineering. Elsevier Ltd, pp. 22–31. https://doi.org/10.1016/j.proeng.2015.09.211.
Hernández-Sandoval, F.E., Del Ángel-Rodríguez, J.A., Núñez-Vázquez, E.J., Band-Schmidt, C.J., Arredondo-Vega, B.O., Campa-Córdova, Á.I., Moreno-Legorreta, M., Fernández-Herrera, L.J., López-Cortés, D.J., 2022. Effects on cell growth, lipid and biochemical composition of Thalassiosira weissflogii (Bacillariophyceae) cultured under two nitrogen sources. Appl. Sci. 12 https://doi.org/10.3390/app12030961.
Hulatt, C.J., Wijffels, R.H., Bolla, S., Kiron, V., 2017. Production of fatty acids and protein by nannochloropsis in flat-plate photobioreactors. PLoS One 12. https://doi.org/10.1371/journal.pone.0170440.
Itzhaki, R.F., Gill, D.M., 1964. A micro-biuret method for estimating proteins. Anal. Biochem. 9, 401–410.
Janssen, J.H., Kastenhofer, J., de Hoop, J.A., Lamers, P.P., Wijffels, R.H., Barbosa, M.J., 2018. Effect of nitrogen addition on lipid productivity of nitrogen starved Nannochloropsis gaditana. Algal Res. 33, 125–132. https://doi.org/10.1016/j.algal.2018.05.009.
Janssen, J.H., Lamers, P.P., de Vos, R.C.H., Wijffels, R.H., Barbosa, M.J., 2019. Translocation and de novo synthesis of eicosapentaenoic acid (EPA) during nitrogen starvation in Nannochloropsis gaditana. Algal Res. 37, 138–144. https://doi.org/10.1016/j.algal.2018.11.025.
Kandasamy, L.C., Neves, M.A., Demura, M., Nakajima, M., 2021. The effects of total dissolved carbon dioxide on the growth rate, biochemical composition, and biomass productivity of nonaxenic microalgal polyculture. Sustainability (Switzerland) 13, 1–10. https://doi.org/10.3390/su13042267.
Kang, S., Heo, S., Lee, J.H., 2019. Techno-economic analysis of microalgae-based lipid production: considering influences of microalgal species. Ind. Eng. Chem. Res. 58, 944–955. https://doi.org/10.1021/acs.iecr.8b03999.
Kumar, R., Hegde, A.S., Sharma, K., Parmar, P., Srivatsan, V., 2022. Microalgae as a sustainable source of edible proteins and bioactive peptides – current trends and future prospects. Food Res. Int. https://doi.org/10.1016/j.foodres.2022.111338.
Kumar, S., Ali Kubar, A., Zhu, F., Shao, C., Cui, Y., Hu, X., Ni, J., Abdur Rehman Shah, M., Ding, S., Mehmood, S., Huo, S., 2023. Sunlight filtered via translucent-colored polyvinyl chloride sheets enhanced the light absorption capacity and growth of Arthrospira platensis cultivated in a pilot-scale raceway pond. Bioresour. Technol. 386 https://doi.org/10.1016/j.biortech.2023.129501.
Leflay, H., Okurowska, K., Pandhal, J., Brown, S., 2020. Pathways to economic viability: a pilot scale and techno-economic assessment for algal bioremediation of challenging waste streams. Environ. Sci. (Camb) 6, 3400–3414. https://doi.org/10.1039/d0ew00700e.
Lestari, R.A.S., Nurlaili, E.P., Kusumo, P., 2019. The effect of carbon dioxide concentration and the dimension of photobioreactor on the growth of microalgae Nannochloropsis sp.. In: AIP Conference Proceedings. American Institute of Physics Inc. https://doi.org/10.1063/1.5098284.
Li, T., Wang, W., Yuan, C., Zhang, Y., Xu, J., Zheng, H., Xiang, W., Li, A., 2020. Linking lipid accumulation and photosynthetic efficiency in Nannochloropsis sp. under nutrient limitation and replenishment. J. Appl. Phycol. 32, 1619–1630. https://doi.org/10.1007/s10811-020-02056-w.
Mahat, K., Jamaluddin, H., Nor, N.A., 2015. The effect of different phosphate concentration on growth, lipid productivity and methyl palmitate methyl ester production by Nannochloropsis oculata. J. Teknol 77, 79–83. https://doi.org/10.11113/jt.v77.6915.
Manisali, A.Y., Sunol, A.K., Philippidis, G.P., 2019. Effect of macronutrients on phospholipid production by the microalga Nannochloropsis oculata in a photobioreactor. Algal Res. 41 https://doi.org/10.1016/j.algal.2019.101514.
Mohammady, N.G.E., El-Khatib, K.M., El-Galad, M.I., Abo El-Enin, S.A., Attia, N.K., El-Araby, R., El Diwani, G., Manning, S.R., 2022. Preliminary study on the economic assessment of culturing Nannochloropsis sp. in Egypt for the production of biodiesel and high-value biochemicals. Biomass Convers. Biorefin. 12, 3319–3331. https://doi.org/10.1007/s13399-020-00878-9.
Moraes, L., Rosa, G.M., Cara, I.M., Santos, L.O., Morais, M.G., Grima, E.M., Costa, J.A.V., Fernández, F.G.A., 2020. Bioprocess strategies for enhancing the outdoor production of Nannochloropsis gaditana: an evaluation of the effects of pH on culture performance in tubular photobioreactors. Bioprocess Biosyst. Eng. 43, 1823–1832. https://doi.org/10.1007/s00449-020-02373-x.
Nogueira, N., Nascimento, F.J.A., Cunha, C., Cordeiro, N., 2020. Nannochloropsis gaditana grown outdoors in annular photobioreactors: operation strategies. Algal Res. 48 https://doi.org/10.1016/j.algal.2020.101913.
Paterson, S., Gómez-Cortés, P., de la Fuente, M.A., Hernández-Ledesma, B., 2023. Bioactivity and digestibility of microalgae Tetraselmis sp. and Nannochloropsis sp. as basis of their potential as novel functional foods. Nutrients. https://doi.org/10.3390/nu15020477.
Quinn, J.C., Yates, T., Douglas, N., Weyer, K., Butler, J., Bradley, T.H., Lammers, P.J., 2012. Nannochloropsis production metrics in a scalable outdoor photobioreactor for commercial applications. Bioresour. Technol. 117, 164–171. https://doi.org/10.1016/j.biortech.2012.04.073.
Rafa, N., Ahmed, S.F., Badruddin, I.A., Mofijur, M., Kamangar, S., 2021. Strategies to produce cost-effective third-generation biofuel from microalgae. Front Energy Res. https://doi.org/10.3389/fenrg.2021.749968.
Rahman, H.A., 2018. Climate Change Scenarios in Malaysia: Engaging the Public Bribery Among Undergraduate Students View Project Youth Involvement in Environmental Issues in Kuala Lumpur and Putrajaya View Project.
Rasdi, N.W., Qin, J.G., 2015. Effect of N:P ratio on growth and chemical composition of Nannochloropsis oculata and Tisochrysis lutea. J. Appl. Phycol. 27, 2221–2230. https://doi.org/10.1007/s10811-014-0495-z.
Razzak, S.A., Ilyas, M., Ali, S.A.M., Hossain, M.M., 2015. Effects of CO2 Concentration and pH on mixotrophic growth of Nannochloropsis oculata. Appl. Biochem. Biotechnol. 176, 1290–1302. https://doi.org/10.1007/s12010-015-1646-7.
Remmers, I.M., Martens, D.E., Wijffels, R.H., Lamers, P.P., 2017. Dynamics of triacylglycerol and EPA production in Phaeodactylum tricornutum under nitrogen starvation at different light intensities. PLoS One 12. https://doi.org/10.1371/journal.pone.0175630.
Schade, S., Meier, T., 2021. Techno-economic assessment of microalgae cultivation in a tubular photobioreactor for food in a humid continental climate. Clean Techn. Environ. Policy 23, 1475–1492. https://doi.org/10.1007/s10098-021-02042-x.
Sforza, E., Calvaruso, C., La Rocca, N., Bertucco, A., 2018. Luxury uptake of phosphorus in Nannochloropsis salina: effect of P concentration and light on P uptake in batch and continuous cultures. Biochem. Eng. J. 134, 69–79. https://doi.org/10.1016/j.bej.2018.03.008.
Shield, R.J., Lupatsch, I., 2012. Algae for Aquaculture and Animal Feeds. Technol. Assess; Theory Pract. 21, 23–37.
Sousa, S.C., Machado, M., Freitas, A.C., Gomes, A.M., Carvalho, A.P., 2022. Can growth of Nannochloropsis oculata under modulated stress enhance its lipid-associated biological properties? Mar. Drugs 20. https://doi.org/10.3390/md20120737.
Stein, J.R., 1979. Handbook of Phycological Methods, Culture Methods & Growth Measurement. Cambridge University Press, London, p. 448.
Strickland, J.D.H., Parsons, T.R., 1972. A Practical Handbook of Seawater Analysis, Second edition. Fisheries Research Board of Canada.
Stunda-Zujeva, A., Zuteris, M., Rugele, K., 2018. Sunlight potential for microalgae cultivation in the mid-latitude region the Baltic states. Agron. Res. 16, 910–916. https://doi.org/10.15159/AR.18.126.
Sui, Y., Muys, M., Vermeir, P., D'Adamo, S., Vlaeminck, S.E., 2019. Light regime and growth phase affect the microalgal production of protein quantity and quality with Dunaliella salina. Bioresour. Technol. 275, 145–152. https://doi.org/10.1016/j.biortech.2018.12.046.
Sun, Y., Huang, Y., Liao, Q., Xia, A., Fu, Q., Zhu, X., Fu, J., 2018. Boosting Nannochloropsis oculata growth and lipid accumulation in a lab-scale open raceway pond characterized by improved light distributions employing built-in planar waveguide modules. Bioresour. Technol. 249, 880–889. https://doi.org/10.1016/j.biortech.2017.11.013.
Tan, M.L., Juneng, L., Tangang, F.T., Chung, J.X., Radin Firdaus, R.B., 2021. Changes in temperature extremes and their relationship with ENSO in Malaysia from 1985 to 2018. Int. J. Climatol. 41, E2564–E2580. https://doi.org/10.1002/joc.6864.
Tang, K.H.D., 2019. Climate change in Malaysia: Trends, contributors, impacts, mitigation and adaptations. Sci. Total Environ. https://doi.org/10.1016/j.scitotenv.2018.09.316.

Tran, N.A.T., Padula, M.P., Evenhuis, C.R., Commault, A.S., Ralph, P.J., Tamburic, B., 2016. Proteomic and biophysical analyses reveal a metabolic shift in nitrogen deprived Nannochloropsis oculata. Algal Res. 19, 1–11. https://doi.org/10.1016/j.algal.2016.07.009.

Varshney, P., Beardall, J., Bhattacharya, S., Wangikar, P.P., 2020. Effect of elevated carbon dioxide and nitric oxide on the physiological responses of two green algae, Asterarcys quadricellulare and Chlorella sorokiniana. J. Appl. Phycol. 32, 189–204. https://doi.org/10.1007/s10811-019-01950-2.

Vázquez-Romero, B., Perales, J.A., Pereira, H., Barbosa, M., Ruiz, J., 2022. Techno-economic assessment of microalgae production, harvesting and drying for food, feed, cosmetics, and agriculture. Sci. Total Environ. 837 https://doi.org/10.1016/j.scitotenv.2022.155742.

Wan Razali, W.A., Evans, C.A., Pandhal, J., 2022. Comparative proteomics reveals evidence of enhanced EPA trafficking in a mutant strain of Nannochloropsis oculata. Front. Bioeng. Biotechnol. 10 https://doi.org/10.3389/fbioe.2022.838445.

Willette, S., Gill, S.S., Dungan, B., Schaub, T.M., Jarvis, J.M., St. Hilaire, R., Omar Holguin, F., 2018. Alterations in lipidome and metabolome profiles of Nannochloropsis salina in response to reduced culture temperature during sinusoidal temperature and light. Algal Res. 32, 79–92. https://doi.org/10.1016/j.algal.2018.03.001.

Zhou, H., Xu, Z., Zhou, L., Zhang, Z., Wang, J., Lan, C.Q., 2023. High cell density culture of Neochloris oleoabundans in novel horizontal thin-layer algal reactor: effects of localized aeration, nitrate concentration and mixing frequency. Biochem. Eng. J. 192 https://doi.org/10.1016/j.bej.2023.108839.